A Flying Gripper Based on Cuboid Modular Robots

Bruno Gabrich[1*], David Saldaña[1*], Vijay Kumar[1], and Mark Yim[1].

***Abstract*— We present a novel flying modular platform capable of grasping and transporting objects. It is composed of four cooperative identical modules where each is based on a quadrotor within a cuboid frame with a docking mechanism. Pairs of modules are able to fly independently and physically connect by matching their vertical edges forming a hinge. Four one degree of freedom (DOF) connections results in a one DOF four-bar linkage that can be used to grasp external objects. In this paper, we propose a decentralized method that allows the Flying Gripper to control its position, attitude and aperture angle. In our experiments, we tested the hovering performance for different aperture angles and with a grasped object. The performance for a closing and opening motion was also verified.**

I. Introduction

In nature, cooperative work allows small insects to manipulate and transport objects often heavier than the individuals. Unlike collaboration on the ground, collaboration in air is more complex because of flight stability. Manipulation using a single flying robot with a serial arm manipulator attached to its body [1], [2], [3], is of growing interest in the robotics research community. However, the attachment of an external mechanism on the aerial vehicle increases the system complexity [4], changing inertia, center of mass and overall weight [5]. In order to avoid these issues, related approaches consider the use of light-weight grippers [6], [7], [8]. Those systems minimize the degrees of freedom (DOF) in order to reduce the system complexity, although, these solutions do not avoid the attachment requirement of an external active mechanism. A recent work considers a novel approach for grasping objects in flight [9], [10]. This paper presents a novel modular aerial platform in which multiple single propelled modules, when attached together, cooperatively form a flying vehicle capable of seizing and grasping objects. The grasping action relies on the actuation of the revolute joints located at each module.

The lift capability of modular quadrotors can be increased through the manual docking of other modules to the original modular configuration [11]. Collaborative manipulation in air is an alternative to reduce the complexity of adding manipulator arms to flying vehicles. Multiple quadrotors, with light-weight grippers, cooperatively work to carry payloads of different geometries and weights [12]. Although, the transporting capability is only guaranteed through the attachment of extra mechanisms and parts.

Fig. 1. The Flying Gripper holding a coffee cup in midair.

In a previous work [13], we studied fast self-assembly algorithms for cuboid modules with rigid connections (face to face). In this work, we study non-rigid connections (edge-to-edge) in midair. This type of connection allows the robots to cooperatively grasp objects, as it can be seen in Fig. 1. Here, four modular flying robots are connected together edge-to-edge with cylindrical magnets. The modules body form links in a four-bar linkage that are able to constrain an object in flight by actuating in a cooperative manner. Unlike previous works, we avoid the addition of extra components and embed the grasping capability to the flying vehicle itself, in which the gripper opening-closing motion relies on the propellers actuation only. The main advantage of this platform is its modular capability. Four quadrotors together can deliver a grasping capability without adding any active mechanism.

The contributions of this paper are twofold. *i)* We present the design and the dynamical model of a novel modular flying gripper. *ii)* We propose a decentralized method to control the attitude and aperture of the Flying Gripper.

II. Design and Mechanical System

In the literature, cages for quadrotors are used to enable collision-safe navigation [14]. In our work, we use a light-weight cage to enclose a quadrotor (see Fig. 2). This cage needs to be resilient and light-weight. Docking capabilities were also added to the mechanical system allowing multiple cages to be connected through the use of permanent magnets [15], [16].

A. Flying Vehicle

In the proposed modular platform we use the Crazyflie 2.0 as the chosen aerial vehicle due to its size and ease in

* Equal contributors.

[1] B. Gabrich, D. Saldaña, V. Kumar and M. Yim are with the GRASP Laboratory, University of Pennsylvania, Philadelphia, PA, USA: {brunot, dsaldana, kumar, yim}@seas.upenn.edu.

The authors gratefully acknowledge the support of the Brazilian agency CAPES. The support of DARPA grant HR00111520020, ONR grants N00014-15-1-2115 and N00014-14-1-0510, ARL grant W911NF-08-2-0004, NSF grant IIS-1426840, NSF grant 1138847, and TerraSwarm, one of six centers of STARnet, a Semiconductor Research Corporation program sponsored by MARCO and DARPA.

Fig. 2. A Flying Modular Robot. Equipped with cylindrical magnets located at the corner of the carbon fiber cages. This docking mechanism allows a one DOF connection between two modules.

making adaptations. The quadrotor itself weights 27g and its dimensions are 92x92x29mm. Its battery life lasts around seven minutes, though in our case battery life time is reduced due to the extra payload. The platform is open-source and open-hardware. The motor mounting was modified from the standard design, we tilted the rotors $\alpha = 15°$. This was necessary as more yaw authority was required to enable grasping as a four-bar. However, adding this tilt reduces the quadrotor lifting thrust by 3% [17].

The light-weight cages are made of carbon fiber rods with 3-D printed connectors made of ABS. The connectors are located at the corners of the cage to form the cuboid shape. The cage weights 8g.

B. Docking mechanism

Axially magnetized cylindrical Neodymium Iron Boron (NdFeB) magnets, with $1/8''$ of diameter and $1/4''$ of thickness are mounted on each corner enabling edge-to-edge connections. The cylindrical magnets have mass 0.377g and are able to generate a force of 0.4 kg in a tangential connection between two of the same magnets. This forms a strong bond when two modules connect in flight. Note that the connections are not rigid - each forms a one DOF hinge.

C. System Motion

The four attached modules results in a one DOF four-bar linkage in addition to the combined position and attitude of the conglomerate (see Fig. 3). The four-bar internal angles are controlled by the yaw attitude ψ_i of each module illustrated in Fig. 3. For example modules 1 and 3 rotate clockwise and robots 2 and 4 rotate counter-clockwise in a coordinated manner.

III. Flying Gripper Model

We formulate our flying mechanism based on two main components defined as follows.

Definition 1 (Module). *A* module *is a flying robot that can move by itself in a three dimensional environment and dock horizontally to other modules by matching the vertical edges.*

Definition 2 (Flying Gripper). *A* flying gripper *is composed of four modules connected as a rotational joint at an edge.*

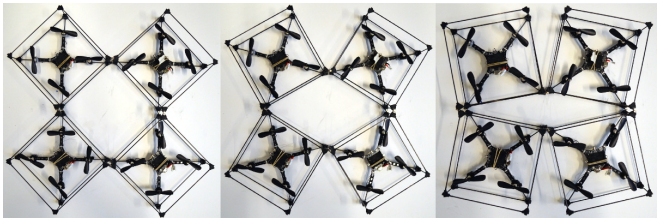

Fig. 3. Flying Gripper motion in a closing procedure; the most left picture shows a 90°of aperture; the center picture shows a 64°of aperture; the most right picture shows a 22°of aperture.

The four connected modules form a four-bar linkage with a inner area as a rhombus shape where the angles of the rhombus can be modified by changing the yaw orientation of the modules.

We consider a group of four modules, indexed by $i = 1, ..., 4$. All modules are homogeneous meaning they have the same shape, inertia, mass and actuators. The location of the ith module relative to the Flying Gripper coordinate frame $\mathcal{G}$ is denoted by $\mathbf{r}_i^{\mathcal{G}} \in \mathbb{R}^3$. The position of the actuator j of the module i written in the module coordinate frame $\mathcal{M}_i$ is denoted as $\mathbf{a}_{ij}^{\mathcal{M}_i} = [x_{ij}^{\mathcal{M}_i}, y_{ij}^{\mathcal{M}_i}, z_{ij}^{\mathcal{M}_i}]^\top$ or as $\mathbf{a}_{ij}^{\mathcal{G}} \in \mathbb{R}^3$ written in the Flying Gripper coordinate frame $\mathcal{G}$. The attitude of the modules are defined by the Euler Angles in which ϕ_i is roll, θ_i is pitch and ψ_i denotes the yaw angle for module i. The inertia tensor of each individual module is defined by $\mathbf{I}$. Along the same lines, the Flying Gripper attitude is defined by ϕ_G, θ_G, ψ_G and its aperture angle by $\gamma \in [0, \pi]$ (see Fig. 4). The Flying Gripper moment of inertia is defined as $\mathbf{J}$.

Our modules are based on a quadrotor platform which has four rotors in a square configuration. Each module i is equipped with four rotors, indexed by $j = 1, ..., 4$, that produce angular speeds ω_{ij} to generate vertical forces

$$f_{ij} = K_f \cos(\alpha)\omega_{ij}^2,$$

and moments

$$M_{ij} = \pm(K_f \sin(\alpha)d + K_m \cos(\alpha))\omega_{ij}^2,$$

where K_f and K_m are motor constants that can be obtained experimentally, d is the distance from the motor j to the module i center of mass, and α is the inclination of the rotor (see the tilted rotors in Fig. 2). Each rotor j from module i is rotated around the vector $\mathbf{a}_{ij}^{\mathcal{M}_i}$. Therefore we can rewrite the forces as

$$f_{ij} = k_f \omega_{ij}^2,$$

and moments

$$M_{ij} = \pm k_m \omega_{ij}^2,$$

where $k_f = K_f \cos(\alpha)$ and $k_m = K_f \sin(\alpha)d + K_m \cos(\alpha)$. The moments are dependent on the direction the propellers spin, which is clockwise or counterclockwise, and on the direction the propellers are tilted. Therefore, propellers 1 and 3 are rotated in a positive direction around its correspondent vector $\mathbf{a}_{ij}^{\mathcal{M}_i}$, while propellers 2 and 4 are rotated in a negative direction.

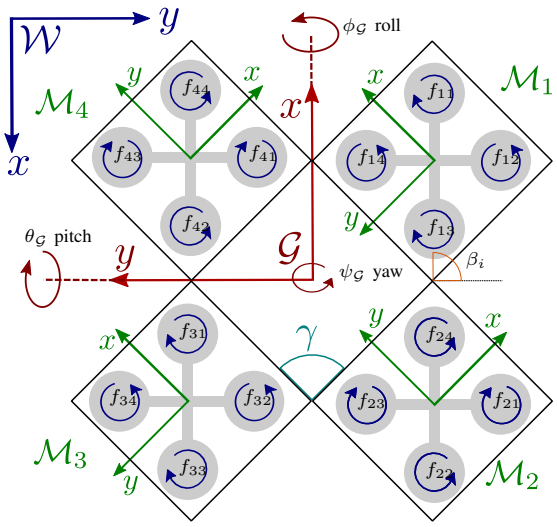

Fig. 4. Representation of the Flying Gripper – the four modules with their respective frames $\mathcal{M}_i$ oriented relative to the Flying Gripper frame $\mathcal{G}$. The Flying Gripper angles are ϕ_G, θ_G, ψ_G , where ϕ_G is the rotation around the x-axis in $\mathcal{G}$, θ_G is the rotation around the y-axis in $\mathcal{G}$ and ψ_G is the rotation around the $z-axis$ in $\mathcal{G}$. The positions of the forces f_{ij} are also illustrated as well as the directions that each propeller spins.

IV. Flying Gripper Dynamics

The Flying Gripper configuration is a specific module formation that enables the opening and closing motion. The variation in the yaw angle of the modules directly changes the aperture angle γ. The total force and moments, can be written in terms of the actuator forces of each individual module in a similar form as the single quadrotor case. Based on the actuator forces, we can write the linear accelerations as

$$4m\ddot{\mathbf{r}}_G = \begin{bmatrix} 0 \\ 0 \\ -4mg \end{bmatrix} + \mathbf{R}_\mathcal{G}^\mathcal{W} \begin{bmatrix} 0 \\ 0 \\ \sum_{ij} f_{ij} \end{bmatrix},$$

where $\mathbf{R}_\mathcal{G}^\mathcal{W}$ is the rotation from the world coordinate frame $\mathcal{W}$ to the Flying Gripper frame $\mathcal{G}$. This transformation is represented by the ZXY Euler angles, where 4 is the total number of modules, m is the mass of each individual module and g is the acceleration of gravity. The rotation from the world coordinate frame $\mathcal{W}$ to the Flying Gripper frame $\mathcal{G}$ is defined as

$$\mathbf{R}_\mathcal{G}^\mathcal{W} = \begin{bmatrix} c\psi c\theta - s\phi s\psi s\theta & -c\phi s\psi & c\psi s\theta + c\theta s\phi s\psi \\ c\theta s\psi + c\psi s\phi s\theta & c\phi c\psi & s\psi s\theta - c\psi c\theta s\phi \\ -c\phi s\theta & s\phi & c\phi c\theta \end{bmatrix}$$

where $c\theta = \cos\theta$, $s\theta = \sin\theta$. Similarly for the angles ϕ and ψ.

The aperture angle γ can be derived based on geometry. Fig. 4 shows a rhombus shape formed in the empty space between modules. Since the shape can be divided into two isosceles triangles, we can write γ in terms of $\psi_i^\mathcal{G}$ as

$$\gamma = 2(-1)^{i+1}\psi_i^\mathcal{G}. \tag{1}$$

Considering the yaw attitude for all modules and its second derivative, we can write the angular acceleration for γ as:

$$\ddot{\gamma} = \frac{1}{2}\sum_{i=1}^{4}(-1)^{i+i}\ddot{\psi}_i^\mathcal{G}.$$

The linearized rotational dynamics in terms of the angular accelerations is given by

$$\mathbf{J}\left[\ddot{\phi}_G, \ddot{\theta}_G, \ddot{\psi}_G, \ddot{\gamma}\right]^\top = \left[M_{xG}, M_{yG}, M_{zG}, T\right]^\top,$$

where $[M_{xG}, M_{yG}, M_{zG}]^\top$ are the Flying Gripper moments and T its closing and opening torque. Due to the addition of an extra DOF the rotational dynamics presents different dimensions compared to the conventional quadrotor dynamics. The matrix $\mathbf{J} \in \mathbb{R}^{4\times4}$ is the Flying Gripper inertia and is defined as follows

$$\mathbf{J} = \begin{bmatrix} \mathbf{I}_G & \mathbf{0} \\ \mathbf{0}^\top & 2I_z \end{bmatrix}$$

where I_z is the inertia around the z-axis for an individual module i. The tensor $\mathbf{I}_G \in \mathbb{R}^{3\times3}$ is the Flying Gripper inertia for roll, pitch and yaw. It can be obtained by

$$\mathbf{I}_G = \sum_{i=1}^{4}\mathbf{I}_i, \tag{2}$$

where $\mathbf{I}_i$ is the contribution of inertia from each module i to the system as a whole. $\mathbf{I}_i \in \mathbb{R}^{3\times3}$ can be computed through the parallel axis theorem and reorienting the inertia of the ith module according to the frame $\mathcal{G}$. Thus, we can write it as

$$\mathbf{I}_i = \mathbf{R}_{\mathcal{M}_i}^\mathcal{G}\mathbf{I}\mathbf{R}_\mathcal{G}^{\mathcal{M}_i} + m\begin{bmatrix} r_{y_i}^2 & 0 & 0 \\ 0 & r_{x_i}^2 & 0 \\ 0 & 0 & \left(r_{x_i}+r_{y_i}\right)^2 \end{bmatrix}, \tag{3}$$

where $\mathbf{I} \in \mathbb{R}^{3\times3}$ is the inertia tensor of the ith module, r_{x_i} and r_{y_i} are the components of the position vector $\mathbf{r}_i = [r_{x_i}, r_{y_i}, r_{z_i}]^\top$, and $\mathbf{R}_{\mathcal{M}_i}^\mathcal{G} \in \mathbb{R}^{3\times3}$ is the rotation matrix from frame $\mathcal{G}$ to frame $\mathcal{M}_i$. Assuming the modules are symmetric, this inertia tensor can be written as $\mathbf{I} = \text{Diag}([I_x, I_y, I_z])$.The rotation matrix can be defined as follows

$$\mathbf{R}_{\mathcal{M}_i}^\mathcal{G} = \begin{bmatrix} \cos\frac{\gamma}{2}(-1)^{i+1} & -\sin\frac{\gamma}{2}(-1)^{i+1} & 0 \\ \sin\frac{\gamma}{2}(-1)^{i+1} & \cos\frac{\gamma}{2}(-1)^{i+1} & 0 \\ 0 & 0 & 1 \end{bmatrix} \tag{4}$$

Then, from (2) and (3) we can compute the Flying Gripper moment of inertia in the x,y,z axis:

$$\mathbf{I}_G = 2\left(\mathbf{R}_{z,\frac{\gamma}{2}}\mathbf{I}\mathbf{R}_{z,\frac{\gamma}{2}}^\top + \mathbf{R}_{z,\frac{\gamma}{2}}^\top\mathbf{I}\mathbf{R}_{z,\frac{\gamma}{2}}\right) +$$

$$m\sum_i \begin{bmatrix} r_{y_i}^2 & 0 & 0 \\ 0 & r_{x_i}^2 & 0 \\ 0 & 0 & \left(r_{x_i}+r_{y_i}\right)^2 \end{bmatrix}.$$

The rotation matrix $\mathbf{R}_{z,\frac{\gamma}{2}} \in \mathbb{R}^{3\times3}$ is a specific case of $\mathbf{R}_{\mathcal{M}_i}^\mathcal{G}$. The inertia considers the position $\mathbf{r}_i^\mathcal{G}$ of each module relative to the Flying Gripper frame $\mathcal{G}$, as well as the transformation $\mathbf{R}_{\mathcal{M}_i}^\mathcal{G}$ for each module i relative to $\mathcal{G}$.

Note that the Flying Gripper moments $[M_{xG}, M_{yG}, M_{zG}, T]^\top$ and total force F_G can be derived

from the forces f_{ij} produced by each rotor j of the ith module. Then, we can describe the resultant moments and total force as

$$\begin{bmatrix} F_G \\ M_{xG} \\ M_{yG} \\ M_{zG} \\ T \end{bmatrix} = \sum_i \begin{bmatrix} 1 & 1 & 1 & 1 \\ -y_{ij}^{\mathcal{G}} & -y_{ij}^{\mathcal{G}} & -y_{ij}^{\mathcal{G}} & -y_{ij}^{\mathcal{G}} \\ x_{ij}^{\mathcal{G}} & x_{ij}^{\mathcal{G}} & x_{ij}^{\mathcal{G}} & x_{ij}^{\mathcal{G}} \\ \frac{k_m}{k_f} & -\frac{k_m}{k_f} & \frac{k_m}{k_f} & -\frac{k_m}{k_f} \\ -p_i & p_i & -p_i & p_i \end{bmatrix} \begin{bmatrix} f_{i1} \\ f_{i2} \\ f_{i3} \\ f_{i4} \end{bmatrix},$$

where $p_i = (-1)^i k_m/k_f$. The positions of the actuators $\mathbf{a}_{ij}^{\mathcal{G}} = [x_{ij}^{\mathcal{G}}, y_{ij}^{\mathcal{G}}, z_{ij}^{\mathcal{G}}]^\top$ are dependent on the aperture angle γ. Given $\mathbf{a}_{ij}^{\mathcal{M}_i} = [x_{ij}^{\mathcal{M}_i}, y_{ij}^{\mathcal{M}_i}, z_{ij}^{\mathcal{M}_i}]^\top$, which is fixed, we apply a transformation to obtain $\mathbf{a}_{ij}^{\mathcal{G}}$

$$\mathbf{a}_{ij}^{\mathcal{G}} = \begin{bmatrix} \mathbf{R}_{\mathcal{M}_i}^{\mathcal{G}} & \mathbf{r}_i^{\mathcal{G}} \end{bmatrix} \begin{bmatrix} \mathbf{a}_{ij}^{\mathcal{M}_i} \\ 1 \end{bmatrix},$$

where $\mathbf{r}_i^{\mathcal{G}}$ is each module i position vector in the Flying Gripper frame $\mathcal{G}$. It can be written as

$$\mathbf{r}_i^{\mathcal{G}} = \frac{w\sqrt{2}}{2} \begin{bmatrix} \sqrt{2}\sin\left(\frac{\pi+(i-1)2\pi}{4}\right)\sqrt{1-\cos\gamma} + \cos\beta_i(\gamma) \\ \sin\beta_i(\gamma) \\ 0 \end{bmatrix},$$

where w is the module width, and $\beta_i(\gamma) \in [\frac{\pi}{4}(-1)^{i+1}, \frac{\pi}{2}(-1)^{i+1}]$ for $i = 1, 2$ and $\beta_i(\gamma) \in [\frac{\pi}{2}(-1)^i, \frac{3\pi}{4}(-1)^i]$ for $i = 3, 4$ (illustrated in Fig. 4). It can be computed as follows

$$\beta_i(\gamma) = \frac{\pi}{4}\left(2\cos i\frac{\pi}{2} + \cos i\pi + 2\sin i\frac{\pi}{2} + \sin i\pi\right) + \frac{\gamma}{2}(-1)^{i+1}$$

In this work one of the objectives is to describe the control of the input commands sent to each one of the motors f_{ij}. Hence, the following section describes our proposed method to control the Flying Gripper attitude and aperture.

V. Flying Gripper Control

The Flying Gripper Control is divided in three stages. Initially we present a centralized trajectory controller that generates a Flying Gripper attitude. Afterwards, we describe the procedure to decentralize the attitude controller to all modules and how the angular accelerations are computed. Later we derive a transformation to generate the control inputs for the j rotor of the module i.

A. Centralized Trajectory Control

The centralized trajectory controller is based in a non-linear controller [18] and assumes the extra degree of freedom γ. Given a desired trajectory in the world frame $\mathbf{r}_G^* = [x_G, y_G, z_G]^\top$ and desired linear velocities $\dot{\mathbf{r}}_G^* = [\dot{x}_G, \dot{y}_G, \dot{z}_G]^\top$ we apply a proportional-derivative controller with a feed-forward term $\ddot{\mathbf{r}}_G = [\ddot{x}_G, \ddot{y}_G, \ddot{z}_G]^\top$ to obtain the desired linear accelerations in the world frame $\ddot{\mathbf{r}}_G^*$

$$\ddot{\mathbf{r}}_G^* = \ddot{\mathbf{r}}_G + \mathbf{K_p}(\mathbf{r}_G^* - \mathbf{r}_G) + \mathbf{K_d}(\dot{\mathbf{r}}_G^* - \dot{\mathbf{r}}_G),$$

where $\mathbf{K_p}$ is the proportional matrix gains represented as $\text{Diag}([K_{p,x}, K_{p,y}, K_{p,z}])$ and the derivative matrix gains is represented by $\mathbf{K_d} = \text{Diag}([K_{d,x}, K_{d,y}, K_{d,z}])$. Given the linear accelerations $\ddot{\mathbf{r}}_G^*$ we can compute the desired attitude $\mathbf{\Theta}_G^* = [\phi_G^*, \theta_G^*, \psi_G^*]^\top$ and desired aperture γ^*, where $\mathbf{\Delta}^* = [\mathbf{\Theta}_G^*, \gamma^*]^\top$, and F_G is the total Flying Gripper force

$$\begin{bmatrix} F_G \\ \mathbf{\Delta}^* \end{bmatrix} = \begin{bmatrix} 4m & 0 & 0 & 0 & 0 \\ 0 & \frac{1}{g}\sin\psi_G & -\frac{1}{g}\cos\psi_G & 0 & 0 \\ 0 & \frac{1}{g}\cos\psi_G & \frac{1}{g}\sin\psi_G & 0 & 0 \\ 0 & 0 & 0 & 1 & 0 \\ 0 & 0 & 0 & 0 & 1 \end{bmatrix} \begin{bmatrix} \ddot{z}_G^* \\ \ddot{x}_G^* \\ \ddot{y}_G^* \\ \psi_G^* \\ \gamma^* \end{bmatrix} + \begin{bmatrix} 4mg \\ 0 \\ 0 \\ 0 \\ 0 \end{bmatrix}$$

where ψ_G is the actual yaw attitude for the Flying Gripper. A centralized behavior $[F_G, \mathbf{\Delta}^*]^\top$ is generated and now it needs to be distributed to all modules.

B. Decentralized Attitude and Aperture Control

In this section, a decentralized attitude and aperture control for the Flying Gripper is described. Initially, the modules receive the desired attitude and aperture $\mathbf{\Delta}^* = [\mathbf{\Theta}_G^*, \gamma^*]^\top$ from the centralized trajectory controller. Thus, given a desired $\mathbf{\Delta}^*$, we can apply a transformation to compute the desired attitude for the ith module $\mathbf{\Theta}_i^*$. This distribution for the desired attitude can be obtained by

$$\mathbf{\Theta}_i^* = \mathbf{D}_i \mathbf{\Delta}^*, \tag{5}$$

where $\mathbf{D}_i \in \mathbb{R}^{3\times 4}$ is the distribution matrix that can be obtained based on the orientation of the ith module relative to $\mathcal{G}$. From (4) and (1), we write the distribution matrix $\mathbf{D}_i$ as

$$\mathbf{D}_i = \begin{bmatrix} \cos\frac{\gamma}{2}(-1)^{i+1} & \sin\frac{\gamma}{2}(-1)^{i+1} & 0 & 0 \\ -\sin\frac{\gamma}{2}(-1)^{i+1} & \cos\frac{\gamma}{2}(-1)^{i+1} & 0 & 0 \\ 0 & 0 & 1 & \frac{(-1)}{2}^{i+1} \end{bmatrix}.$$

This desired attitude $\mathbf{\Theta}_i^*$ for each individual module can be obtained in a decentralized manner. Each module can also use a proportional-derivative controller to compute the angular accelerations

$$\begin{aligned} \ddot{\phi}_i &= K_{p,\phi}(\phi_i^* - \phi_i) + K_{d,\phi}(\dot{\phi}_i^* - \dot{\phi}_i) \\ \ddot{\theta}_i &= K_{p,\theta}(\theta_i^* - \theta_i) + K_{d,\theta}(\dot{\theta}_i^* - \dot{\theta}_i) \\ \ddot{\psi}_i &= K_{p,\psi}(\psi_i^* - \psi_i) + K_{d,\psi}(\dot{\psi}_i^* - \dot{\psi}_i) \end{aligned}$$

where K_p, K_d are constant positive gains. We can rewrite this proportional-derivative controller in a compact form

$$\dot{\mathbf{\Omega}}_i^{\mathcal{M}_i} = \mathbf{K_{p,\Theta}}(\mathbf{\Theta}_i^* - \mathbf{\Theta}_i) + \mathbf{K_{d,\Omega}}(\mathbf{\Omega}_i^* - \mathbf{\Omega}_i) \tag{6}$$

where $\dot{\mathbf{\Omega}}_i^{\mathcal{M}_i}$ is the desired angular acceleration of the ith module in its coordinate frame $\mathcal{M}_i$. The diagonal matrices $\mathbf{K_{p,\Theta}} = \text{Diag}([K_{p,\phi}, K_{p,\theta}, K_{p,\psi}])$ and $\mathbf{K_{d,\Omega}} = \text{Diag}([K_{d,\phi}, K_{d,\theta}, K_{d,\psi}])$ contains the proportional and derivative gains constants respectively. The desired angular velocity can either come from the trajectory or be equal to zero $\mathbf{\Omega}_i^* = \mathbf{0}$.

Given a desired Flying Gripper attitude and aperture $\mathbf{\Delta}^*$, we are able to obtain each module angular acceleration $\dot{\mathbf{\Omega}}_i^{\mathcal{M}_i}$. Those accelerations are calculated in each module frame, although each module needs to compute the control inputs for their motors based on the Flying Gripper frame $\mathcal{G}$. We then apply the following transformation

$$\dot{\mathbf{\Omega}}_i^{\mathcal{G}} = \mathbf{R}_{\mathcal{M}_i}^{\mathcal{G}} \dot{\mathbf{\Omega}}^{\mathcal{M}_i}, \tag{7}$$

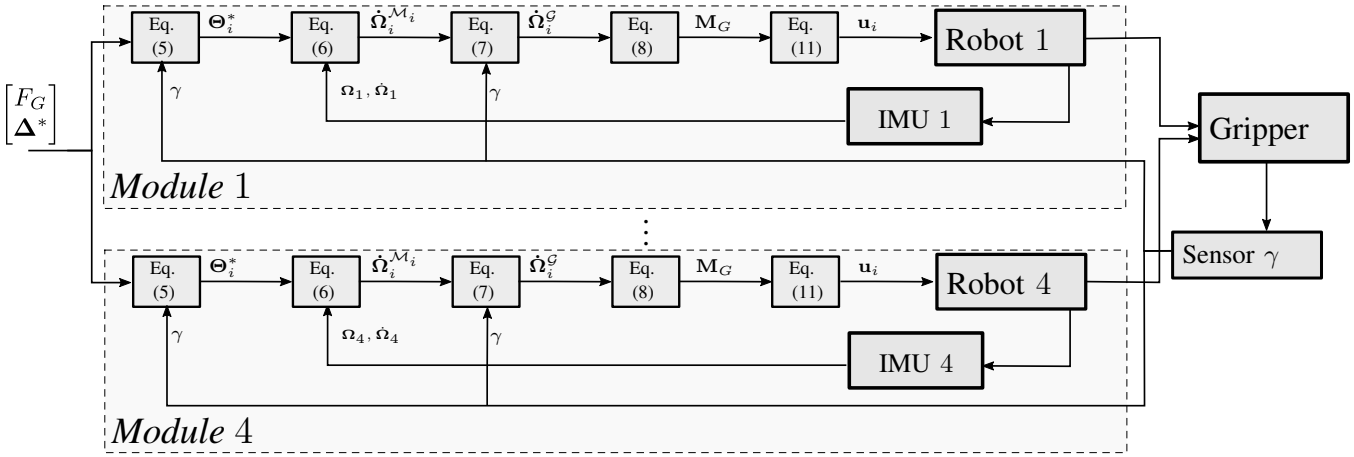

Fig. 5. Diagram of the decentralized attitude controller. The dashed boxes represent the modules and their internal distributed controller. The modules use the feedback from their own IMU and the aperture angle γ from an external observer.

where $\dot{\mathbf{\Omega}}_i^{\mathcal{G}}$ is the angular acceleration of the ith module with respect to the frame $\mathcal{G}$. Using the obtained $\dot{\mathbf{\Omega}}_i^{\mathcal{G}}$, we can compute the moments for the Flying Gripper based on the angular acceleration of the ith module. Then we have,

$$\mathbf{M}_G = \mathbf{I}_G \dot{\mathbf{\Omega}}_i^{\mathcal{G}} \tag{8}$$

where $\mathbf{M}_G = [M_{xG}, M_{yG}, M_{zG}]^\top$.

The last step of the controller is to distribute the forces for each module i and rotor j. First, we assume that each module behaves as a single propeller, then we denote the force for the ith module by F_i. We can divide the thrust F_G and moments $\mathbf{M}_G$ (from (8)) into the four modules as

$$F_i = \frac{F_G}{4} + \frac{M_{xG}}{4r_{y_i}} + \frac{M_{yG}}{4r_{x_i}} \pm \frac{k_f}{4k_m} M_{zG}. \tag{9}$$

Since the Flying Gripper is over-actuated there are multiple solutions to control the flying platform. In this work, we use the one that guarantees equal forces for the rotors in the module i. This approach is relevant for our platform since the maximum actuation generated by one single rotor is very limited. Therefore, to compute the forces for the rotor j of the module i, we apply $f_{ij} = F_i/4$. From (9), we can write f_{ij} as

$$f_{ij} = \frac{1}{16}(F_G + \frac{M_{xG}}{r_{y_i}} + \frac{M_{yG}}{r_{x_i}} + (-1)^{(j+1)} \frac{k_f}{k_m} M_{zG}) \tag{10}$$

Therefore, we define $\mathbf{u}_i = [f_{i1}, f_{i2}, f_{i3}, f_{i4}]^\top$ as the control inputs to the rotors for module i. We can compute it as

$$\mathbf{u}_i = \mathbf{C}_i \begin{bmatrix} F_G \\ \mathbf{I}_G \dot{\mathbf{\Omega}}_i^{\mathcal{G}} \end{bmatrix}, \tag{11}$$

where $\mathbf{C}_i \in \mathbb{R}^{4\times4}$ is the input control matrix that converts the total system force and accelerations into control inputs for the actuators. It can be defined by

$$\mathbf{C}_i = \frac{1}{16} \begin{bmatrix} 1 & \frac{1}{r_{y_i}} & \frac{1}{r_{x_i}} & \frac{k_f}{k_m} \\ 1 & \frac{1}{r_{y_i}} & \frac{1}{r_{x_i}} & -\frac{k_f}{k_m} \\ 1 & \frac{1}{r_{y_i}} & \frac{1}{r_{x_i}} & \frac{k_f}{k_m} \\ 1 & \frac{1}{r_{y_i}} & \frac{1}{r_{x_i}} & -\frac{k_f}{k_m} \end{bmatrix}. \tag{12}$$

We highlight that our approach distributes the gripper desired state $[F_G, \mathbf{\Delta}^*]^\top$ to the four modules, and they independently compute their control input $\mathbf{u}_i$. The decentralized attitude controller is summarized in Fig. 5. We can see that all robots receive the same attitude and aperture command. Using, the local IMU and the γ feedback from the external observer, the robot can compute its own control input. The resultant action of each module drives the gripper to the desired state $[F_G, \mathbf{\Delta}^*]^\top$.

VI. Experiments

In these experiments, we want to validate dynamic aspects of the Flying Gripper. These include: actuating the aperture degree of freedom, carrying a payload and hovering with different aperture angles.

We used the Crazyflie-ROS node [19] to control the modules, and to determine the Flying Gripper pose and aperture angle. A motion capture system (VICON) operated at 100 Hz is used to obtain the pose of the robot along with providing the actual γ angle. Each module locally measures its angular velocities using its IMU. All control commands are computed in ROS and sent to the robot via 2.4GHz radio. Visual-Inertial Odometry (VIO) could be used to estimate the conglomerate position in space through the attachment of a small camera, and other sensors could be used to estimate the angle γ. Although, these solutions increase complexity, consequently delaying the development of a novel system.

The original crazyflie firmware was modified to implement equations (5) and (7). The trajectory is calculated in a computer, it sends attitude commands and the aperture angle through radio communication. The attitude commands are sent at 50Hz and the current aperture angle at 5Hz. Because the modules do not share the same orientation for most cases of operation (except $\gamma = 0°$), one of the main challenges in the experiments was being able to control the attitude of the gripper using the local IMU sensors. However, the proposed attitude controller uses the observed γ to allow the robot adapt its measurements and actuation.

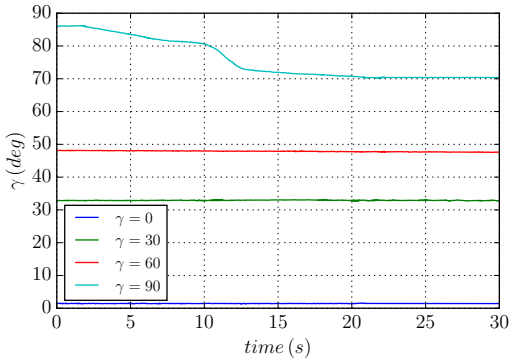

Fig. 6. Hovering with different aperture angles.

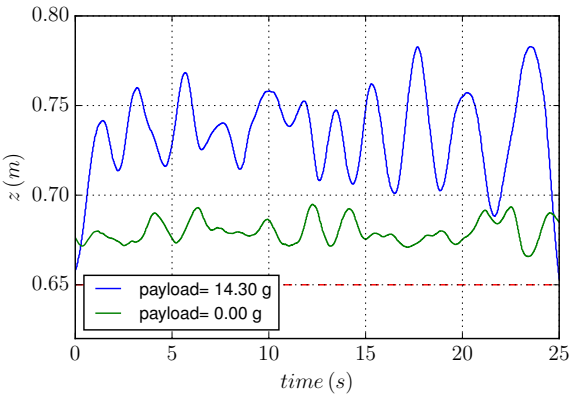

Fig. 7. Hovering with and without a coffee cup.

A. Hovering for specific γ apertures

Initially we want to evaluate the behavior of the Flying Gripper for a hover condition. The robots try to maintain a given aperture angle γ during flight. The Flying Gripper hovers at $z = 0.65$m from the ground.

In Fig. 6, we can see the gripper maintains various initial aperture angles over time open-loop. The only exception is the case of $90°$, where the aperture drifts from $90°$ to $71°$. Sometimes we notice a heterogeneous behavior during takeoff, where we see some modules taking off a couple of milliseconds before or after an adjacent module. Whenever it happens, each module attitude controller tries to correct and stabilize in different proportions. Consequently, reaction forces acts on the flying vehicle causing, for specific cases, an angle drift for the open-loop case.

B. Hovering with and without a payload

The Flying Gripper behavior under an additional payload is verified with the gripper constraining a simple cup. Fig. 7 illustrates both cases with and without payload and the impact on altitude. We can see the extra load generates higher oscillations in the z-axis in comparison to the no-payload case. The bigger amplitudes for the payload case is justifiable since the hovering controller is trying to compensate for the extra weight, but overshoots.

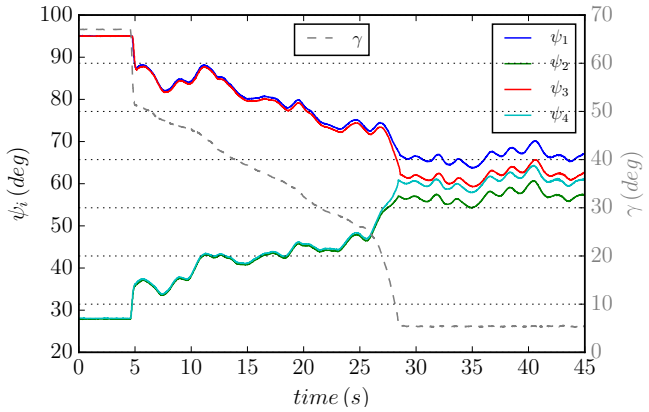

Fig. 8. Closing the gripper. The plot shows the change of the yaw angle of the modules (continuous lines) while the aperture angle is reducing (dashed line).

C. Gripper actuation

The aperture angle γ is controlled in midair. The gripper is being actuated through an aperture angle under closed-loop control. The result of closing the gripper in midair can be seen in Fig. 8. It illustrates how the modules change their yaw orientation to progressively reduce the aperture of the gripper. We know that all modules have approximately the same orientation when the gripper is closed. Then, we can see this exact behavior after second 30, where the robots achieve the same orientation as the gripper. Although the control of the yaw and the aperture angles are coupled, we can see that the orientation of the gripper was maintained as the robots closed the gripper, meaning the aperture angle was changing towards to $0°$.

An important capability of the Flying Gripper is being able to change the aperture angle without compromising the stability and at the same time maintaining at a desired location in space. Fig. 9 illustrates how the griper can progressively close the aperture angle without affecting the altitude. The aperture angle was actuated from $68°$ to $0°$ and the time-response of this actuation was around 25 seconds. We also notice that the altitude remains approximately constant. Therefore, we conclude that the system is capable to accurately approach an object at a specific height and grasp it.

D. Yaw Actuation

The initial experiments were conducted with propellers oriented parallel to the ground during hover. For the Crazyflie 2.0, the moments generated to actuate the aperture angle γ by the normal method of differential velocities between diagonal propeller pairs were not strong enough. To increase the controllable yaw moment, we tilted the propellers $15°$ as in [17]. This created 3 times more yaw-control action allowing the gripper to generate enough moments to execute the grasping procedure.

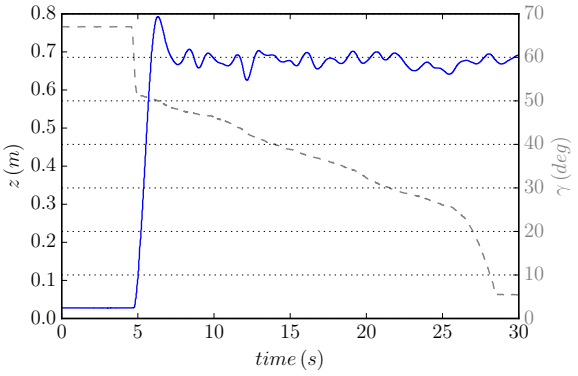

Fig. 9. Altitude vs γ. The plot shows the behavior of the altitude of the gripper (continuous line) while the aperture angle is being reduced (dashed line).

E. Grasping procedure

The main application of the gripper is transporting objects from one place to another. In our experiments, we moved a coffee cup from a conic support to a trash can. The conic support keeps the coffee cup in a static location avoiding undesired motions due to the air flow. We use the centralized trajectory control to follow a set of way points including the desired aperture angle for each way point. Joining the attitude controller and the desired aperture, we use the control architecture (summarized in Fig. 5) to drive the modular gripper. As we can see in the attached video, for any initial location, we define five way points. *i)* A small distance (0.2m) above the coffee cup with maximum aperture (90°). *ii)* Coffee cup location with the maximum aperture (90°). This motion avoids collisions with the coffee cup during the grasping process. *iii)* Coffee cup location with an small aperture (35°). The aperture is known priory and is sufficient to grasp the coffee cup. *iv)* A distance of 0.4m over the trash can location maintaining the small aperture (35°). This transports the object in midair. *v)* Same location and larger angle (60°). Opening the aperture angle releases the coffee cup and makes it fall by gravity at the desired location.

VII. Conclusion and Future Work

In this paper, we introduced a novel flying platform based on modular robots capable of grasping and transporting objects. The Flying Gripper is able to perform this task by decentralizing the attitude and aperture control. We proposed a decentralized controller to allow four modular robots to cooperatively fly and change the aperture angle in midair. Through multiple experiments, we show that our platform is able to execute the grasping and transporting tasks.

In future work we aim to explore the scalability of the system, using n number of modules possibly with docking in midair. Forming the Flying Gripper in midair is a very hard task because the connections are non-rigid. We also want to study the grasping and holding forces. Since this forces are coupled with thrust force, it is a problem that deserves attention.

References

[1] S. Kim, S. Choi, and H. J. Kim, "Aerial manipulation using a quadrotor with a two dof robotic arm," in *Intelligent Robots and Systems (IROS), 2013 IEEE/RSJ International Conference on*. IEEE, 2013, pp. 4990–4995.

[2] F. Huber, K. Kondak, K. Krieger, D. Sommer, M. Schwarzbach, M. Laiacker, I. Kossyk, S. Parusel, S. Haddadin, and A. Albu-Schäffer, "First analysis and experiments in aerial manipulation using fully actuated redundant robot arm," in *Intelligent Robots and Systems (IROS), 2013 IEEE/RSJ International Conference on*. IEEE, 2013, pp. 3452–3457.

[3] C. D. Bellicoso, L. R. Buonocore, V. Lippiello, and B. Siciliano, "Design, modeling and control of a 5-dof light-weight robot arm for aerial manipulation," in *Control and Automation (MED), 2015 23th Mediterranean Conference on*. IEEE, 2015, pp. 853–858.

[4] A. Q. Keemink, M. Fumagalli, S. Stramigioli, and R. Carloni, "Mechanical design of a manipulation system for unmanned aerial vehicles," in *Robotics and Automation (ICRA), 2012 IEEE International Conference on*. IEEE, 2012, pp. 3147–3152.

[5] R. Oung and R. D'Andrea, "The distributed flight array," *Mechatronics*, vol. 21, no. 6, pp. 908–917, 2011.

[6] D. Mellinger, Q. Lindsey, M. Shomin, and V. Kumar, "Design, modeling, estimation and control for aerial grasping and manipulation," in *Intelligent Robots and Systems (IROS), 2011 IEEE/RSJ International Conference on*. IEEE, 2011, pp. 2668–2673.

[7] Q. Lindsey, D. Mellinger, and V. Kumar, "Construction of cubic structures with quadrotor teams," *Proc. Robotics: Science & Systems VII*, 2011.

[8] P. E. Pounds, D. R. Bersak, and A. M. Dollar, "Grasping from the air: Hovering capture and load stability," in *Robotics and Automation (ICRA), 2011 IEEE International Conference on*. IEEE, 2011, pp. 2491–2498.

[9] M. Zhao, K. Kawasaki, X. Chen, S. Noda, K. Okada, and M. Inaba, "Whole-body aerial manipulation by transformable multirotor with two-dimensional multilinks," in *Robotics and Automation (ICRA), 2017 IEEE International Conference on*. IEEE, 2017, pp. 5175–5182.

[10] M. Zhao, K. Kawasaki, X. Chen, Y. Kakiuchi, K. Okada, and M. Inaba, "Transformable multirotor with two-dimensional multilinks: Modeling, control, and whole-body aerial manipulation," in *International Symposium on Experimental Robotics*. Springer, 2016, pp. 515–524.

[11] M. J. Duffy and A. Samaritano, "The lift! project-modular, electric vertical lift system with ground power tether," in *33rd AIAA Applied Aerodynamics Conference*, 2015, p. 3013.

[12] D. Mellinger, M. Shomin, N. Michael, and V. Kumar, "Cooperative grasping and transport using multiple quadrotors," *Springer Tracts in Advanced Robotics*, vol. 83 STAR, pp. 545–558, 2012.

[13] D. Saldaña, B. Gabrich, M. Whitzer, A. Prorok, M. F. Campos, M. Yim, and V. Kumar, "A decentralized algorithm for assembling structures with modular robots," in *2017 IEEE/RSJ International Conference on Intelligent Robots and Systems (IROS)*.

[14] Y. Mulgaonkar, T. Kientz, M. Whitzer, and V. Kumar, "Design and fabrication of safe, light-weight, flying robots," in *ASME 2015 International Design Engineering Technical Conferences and Computers and Information in Engineering Conference*. American Society of Mechanical Engineers, 2015, pp. V05BT08A021–V05BT08A021.

[15] J. W. Romanishin, K. Gilpin, and D. Rus, "M-Blocks : Momentum-driven , Magnetic Modular Robots," pp. 4288–4295, 2013.

[16] J. Davey, N. Kwok, and M. Yim, "Emulating self-reconfigurable robots-design of the smores system," in *2012 IEEE/RSJ International Conference on Intelligent Robots and Systems*. IEEE, 2012, pp. 4464–4469.

[17] D. Falanga, E. Mueggler, M. Faessler, and D. Scaramuzza, "Aggressive quadrotor flight through narrow gaps with onboard sensing and computing using active vision," in *Proc. of the IEEE International Conference on Robotics and Automation (ICRA)*, 2017.

[18] N. Michael, D. Mellinger, Q. Lindsey, and V. Kumar, "The grasp multiple micro-uav testbed," *IEEE Robotics & Automation Magazine*, vol. 17, no. 3, pp. 56–65, 2010.

[19] W. Hoenig, C. Milanes, L. Scaria, T. Phan, M. Bolas, and N. Ayanian, "Mixed reality for robotics," in *Intelligent Robots and Systems (IROS), 2015 IEEE/RSJ International Conference on*. IEEE, 2015, pp. 5382–5387.